Activated Carbons Impregnated with Na_2S and H_2SO_4: Texture, Surface Chemistry and Application to Mercury Removal from Aqueous Solutions

Z. Abdelouahab-Reddam, A. Wahby, R. El Mail, J. Silvestre-Albero, F. Rodríguez- Reinoso and A. Sepúlveda-Escribano

Reprinted from

Adsorption Science & Technology

2014 Volume 32 Number 2&3

Multi-Science Publishing Co. Ltd.
5 Wates Way, Brentwood, Essex CM15 9TB, United Kingdom

Activated Carbons Impregnated with Na_2S and H_2SO_4: Texture, Surface Chemistry and Application to Mercury Removal from Aqueous Solutions

Z. Abdelouahab-Reddam[1,2], A. Wahby[1,2], R. El Mail[2], J. Silvestre-Albero[1], F. Rodríguez-Reinoso[1] and A. Sepúlveda-Escribano[1,*] *(1) Laboratorio de Materiales Avanzados, Departamento de Química Inorgánica, Instituto Universitario de Materiales de Alicante, Universidad de Alicante, Apartado 99, E-03080, Alicante, Spain. (2) Equipe de Recherche Chimie de l'Eau et Pollution Atmosphérique, Département de Chimie, Faculté des Sciences, Université Abdelmalek Essaadi, Tétouan, Morocco.*

(Received date: 16 September 2013; Accepted date: 22 January 2014)

ABSTRACT: The effects of treatment of an activated carbon with sulphur precursors on its textural properties and on the ability of the complex synthesized for mercury removal in aqueous solutions are studied. To this end, a commercial activated carbon has been modified by treatments with aqueous solutions of Na_2S and H_2SO_4 at two temperatures (25 and 140 °C) to introduce sulphur species on its surface. The prepared adsorbents have been characterized by N_2 (–196 °C) and CO_2 (0 °C) adsorption, thermogravimetric analysis, temperature-programmed decomposition and X-ray photoelectron spectroscopy, and their adsorption capacities to remove Hg(II) ions in aqueous solutions have been determined. It has been shown that the impregnation treatments slightly modified the textural properties of the samples, with a small increase in the textural parameters (BET surface area and mesopore volumes). By contrast, surface oxygen content was increased when impregnation was carried out with Na_2S, but it decreased when H_2SO_4 was used. However, the main effect of the impregnation treatments was the formation of surface sulphur complexes of thiol type, which was only achieved when the impregnation treatments were carried out at low temperature (25 °C). The presence of surface sulphur enhances the adsorption behaviour of these samples in the removal of Hg(II) cations in aqueous solutions at pH 2. In fact, complete Hg(II) removal is only obtained with the sulphur-containing activated carbons.

1. INTRODUCTION

Mercury is one of the most dangerous heavy metals for both humans and the environment (Griffiths *et al*. 2006). Upon reaching the food chain, mercuric compounds are accumulated in animal and plant tissues. Mercuric compounds are widely used in many industries, depending on their physical and the chemical properties. In fact, the most important application of metallic mercury is in the manufacture of chlorine and sodium hydroxide. It is also used in the chemical industry for the manufacture of batteries and mercury electrodes. It is even used in the manufacture of mercury-based electrical capacitors, as well as in the development of anticorrosive cinnabar-based paints. Mercuric compounds are also used in the petrochemical industry (Lee *et al*. 2006). Increasingly, industrial applications of mercury are sloping owing its high toxicity.

Mercury can be absorbed into the human body by different pathways, and the mode of absorption strongly depends on its chemical form and the route of entry, which can be either

*Author to whom all correspondence should be addressed. E-mail: asepul@ua.es (A. Sepúlveda-Escribano).

through ingestion or inhalation. The metal is easily accumulated in the living tissues, especially in the brain (Barán 1994). At highly toxic levels, mercury is one of the priority pollutants listed by the U.S. Environmental Protection Agency (USEPA), because it can pass through the blood-brain barrier and can also affect foetal brain (Zabihi *et al*. 2009). Previous studies have shown that high concentrations of Hg(II) causes impairment of pulmonary and renal functions, chest pain and dyspnoea (Berglund and Bertin 1969; Krishna-Murti and Vishwanathan 1991). According to the USEPA guidelines, the maximum concentration of mercury in drinking water should only be 2 μg/l, while its concentration in the waste discharge should be less than 10 μg/l (USEPA 2007; Wajima and Sugawara 2011).

To reduce pollution caused by heavy metals, several techniques are currently available, such as precipitation (Mauchauffée and Meux 2007), reverse osmosis (Mohsem-Nia *et al*. 2007), ion exchange (Verma *et al*. 2008), coagulation (El Samrani *et al*. 2008) and adsorption using porous sorbents (Gupta *et al*. 2003). The latter is generally considered to be an appropriate technology for the treatment of the effluents with a high level of pollution load, especially, in cases involving contamination with mercury (Manchester *et al*. 2008). In particular, adsorption on activated carbon has been among the most effective removal techniques for decades (McKay and Bino 1990; Kadirvelu *et al*. 2004).

Different treatment methods have been used to modify the surface and/or the textural properties of activated carbons to improve its adsorption capacity. In this sense, sulphur impregnation has been shown to greatly enhance adsorption of mercury on activated carbons. Several studies have reported the positive effect of impregnation of activated carbon with sulphur in the adsorption of both organic and inorganic forms of mercury. The increasing adsorptive capacity of the sulphurized activated carbons is attributed to the high affinity of mercury for sulphur, which generates more active sites on the surface of activated carbon for selective adsorption of mercury (Wajima and Sugawara 2011; Hsi and Chen 2012; Ie *et al*. 2013; Pillay *et al*. 2013). According to several works related to the modification of activated carbons with sulphur, the mercury adsorption capacity of the obtained material depends mainly on the impregnation temperature, the nature and the amount of the impregnating agent used (Wei *et al*. 1998; Wenguo *et al*. 2006). Yuan et al. (2004) have studied the impregnation of activated carbons with Na_2S at 140 °C. The obtained results showed that the amount of sulphur fixed on the carbon surface is proportional to the concentration of sulphur used in the impregnation process. However, it was shown that the surface area of the activated carbons decreased from 579 to 470 m^2/g. These results establish that during the impregnation process, Na_2S molecules occupy the active surface sites of activated carbon and, consequently, lead to a reduction of the surface area. Thus, the optimization of the sulphur amount used is deemed necessary. Several studies demonstrate the effectiveness of such treatment in the process of vapour-phase mercury removal (Otani *et al*. 1988; Krishnan *et al*. 1994; Karatza *et al*. 1996). Nevertheless, those emphasizing its application in the liquid phase remain rather limited. In this sense, the aim of this paper is to study the influence of a sulphur-modification treatment of activated carbons on their structural/textural properties, as well as the application of the modified materials in the removal of mercury from aqueous solution.

2. EXPERIMENTAL ANALYSIS

2.1. Preparation of Samples

A commercial granular activated carbon (UAC; DARCO 12X40, NORIT Americas Inc.) was modified by impregnation with solutions of Na_2S and H_2SO_4 at two different concentrations, at 25 and 140 °C.

2.1.1. Impregnation with Na_2S

The impregnation protocol used was based on that reported by Yuan *et al*. (2004), although they only used impregnation at high temperature (140 °C). Thus, two samples of UAC (approximately 0.5 g) were immersed into 200 ml of an aqueous solution of Na_2S, prepared using 0.5 and 7.5 g of sodium sulphide, respectively. The impregnation treatment was performed at two different temperatures, namely, at 25 and 140 °C. The samples were kept immersed for 24 hours with moderate stirring. Once impregnated, the samples were filtered under vacuum and then dried at 120 °C for 24 hours. The dried samples were thermally treated at 700 °C, under inert atmosphere, with a nitrogen flow of 100 ml/minute for 2 hours. The prepared samples were labelled as $ACSS_{(xxg\text{-}yy\ °C)}$, with 'xx' being the amount of Na_2S used and 'yy' being the impregnation temperature. Thus, the sample $ACSS_{(0.5g\text{-}140\ °C)}$ represents the activated carbon impregnated at 140 °C with a solution containing 0.5 g of Na_2S.

2.1.2. Impregnation with H_2SO_4

In this case, the impregnation method was similar to that used by Guo *et al*. (2005). However, the use of sulphuric acid as a post-activation agent and the temperature used (140 °C) are an original contribution of the present work. The experimental procedure is identical to that described in the 'Impregnation with Na_2S' section. Thus, two UAC samples were immersed into 200 ml of an aqueous solution of H_2SO_4 with 5% and 40% (vol/vol), respectively. Likewise, the impregnation treatment was carried out at 25 and 140 °C for 24 hours with moderate stirring. Subsequently, the impregnated samples were recovered after vacuum filtration, dried at 120 °C for 24 hours and heated up to 700 °C, under nitrogen flow (100 ml/minute), during a soaking time of 2 hours. Samples were labelled as $ACSA_{(xx\%\text{-}yy\ °C)}$, with 'xx' being the concentration of the sulphuric acid solution used and 'yy' being the impregnation temperature.

2.2. Characterization of Samples

The optimal heat-treatment temperature for sulphur fixation was determined by thermogravimetric (TG) analysis, which was performed using a thermobalance (SDT 2960 Simultaneous DSC-TGA; TA instruments). The study of the decomposition temperature of the untreated carbon (UAC) was carried out under an inert atmosphere (nitrogen flow of 100 ml/minute) over the whole temperature range 25–1000 °C and with a heating rate of 10 °C/minute. Thus, approximately 10 mg of the sample was heated up to 1000 °C and the weight loss was recorded as a function of temperature.

The textural properties of the untreated activated carbon and all the modified carbons were determined by N_2 and CO_2 adsorption at –196 and 0 °C, respectively, using a fully automated home-made manometric equipment (LMA-Sorb; Silvestre-Albero *et al*. 2009). Before performing the measurements, the sample was outgassed at 250 °C for 4 hours under vacuum (10^{-7} bar). The 'apparent' surface area (Gregg and Sing 1982) was calculated applying the BET method to the N_2 adsorption data (Martín-Martínez 1990) in the relative pressure range between 0.05 and 0.18. The total volume of micropores (V_0) was obtained by applying the Dubinin–Radushkevich equation (DR) to the nitrogen adsorption data. The volume corresponding to the narrow porosity (V_n) was calculated by applying the DR equation to the CO_2 adsorption data (Garrido *et al*. 1987). The total volume of pores (V_t) was estimated from the N_2 adsorption isotherm. It corresponds to the amount adsorbed at the relative pressure $P/P_0 = 0.95$. Finally, the mesoporous volume (V_{meso}) was obtained as $V_t - V_0$.

The temperature-programmed decomposition (TPD) analysis was performed using a quartz U-shaped reactor containing approximately 10 mg of sample. It was heated from room temperature (25 °C) to 1000 °C with a heating rate of 10 °C/minute, under helium flow (50 ml/minute). The evolved gases were analyzed by a quadrupole mass spectrometer (OmniStar TM PFEIFFER VACUUM) connected online.

The X-ray photoelectron spectroscopy (XPS) analysis was performed using a VG-Microtech Multilab 3000 spectrometer equipped with a hemispherical electron analyzer and a Mg-K_α (h = 1253.6 eV; 1 eV = $1.6302 \times \cdot 10^{-19}$ J) 300-W X ray source. The powder samples were pressed into small Inox cylinders, which were mounted on a sample rod placed in a pre-treatment chamber before being transferred to the analysis chamber. Before recording the spectrum, the sample was maintained in the analysis chamber until a residual pressure of approximately $5 \times \cdot 10^{-7}$ N·m^{-2} was reached. The spectra were collected at pass energy of 50 eV. The intensities were estimated by calculating the integral of each peak, after subtracting the S-shaped background, and fitting the experimental curve to a combination of Lorentzian (30%) and Gaussian (70%) lines. All binding energies were referenced to the C 1s line at 284.6 eV, which provided binding energy values with an accuracy of ±0.2 eV.

It should be mentioned that for all the characterization techniques used in this study, three analyzes were performed for each sample, and only the mean values are reported.

2.3. Mercury Adsorption Measurements

The carbon samples were dried at 100 °C for 4 hours under vacuum to remove the eventually adsorbed water (Jayson *et al*. 1984). To evaluate the Hg(II) adsorption capacity for the different carbon materials, an aqueous solution of Hg(II), with a concentration of 20 mg/l, was prepared from $HgCl_2$ in hydrochloride acid with a pH value of 2. Previous studies report that in the presence of Cl^-, the predominant Hg species at pH < 4 is Hg(II) (Yardim *et al*. 2003). The mercury adsorption measurements were performed by contacting 0.5 g of the evaluated sample with 100 ml of the prepared solution for a period of 5–24 hours at room temperature, with a constant agitation rate of 200 rpm, in a shaker bath. The contact time was selected on the basis of previous studies (Mohan *et al*. 2001). The suspensions were filtered through a microporous filter before the determination of the amount of Hg(II) in solution, which was accomplished spectrophotometrically with an ATI Unicam UV–VIS spectrometer, at 230 nm (Nabais *et al*. 2006).

All the adsorption experiments were performed in triplicate and the average of the obtained concentrations is reported.

3. RESULTS AND DISCUSSION

3.1. TG Measurements

To accomplish the process of sulphur fixation on the activated carbon surface, the impregnation step is usually followed by a heat treatment. The latter is rather problematic in the case of activated carbons, mainly because of the decomposition of the oxygen surface groups and the bulk, at higher temperatures. Thus, thermal decomposition of the untreated activated carbon used as a starting material (UAC), under inert atmosphere (nitrogen), which was monitored by TG-derivative thermogravimetric (TG-DTG) analysis. Figures 1(a and b) show the TG and DTG profiles, respectively, of UAC, $ACSS_{(7.5g\text{-}140\ °C)}$, $ACSA_{(40\%\text{-}25\ °C)}$ and $ACSA_{(40\%\text{-}140\ °C)}$. The original

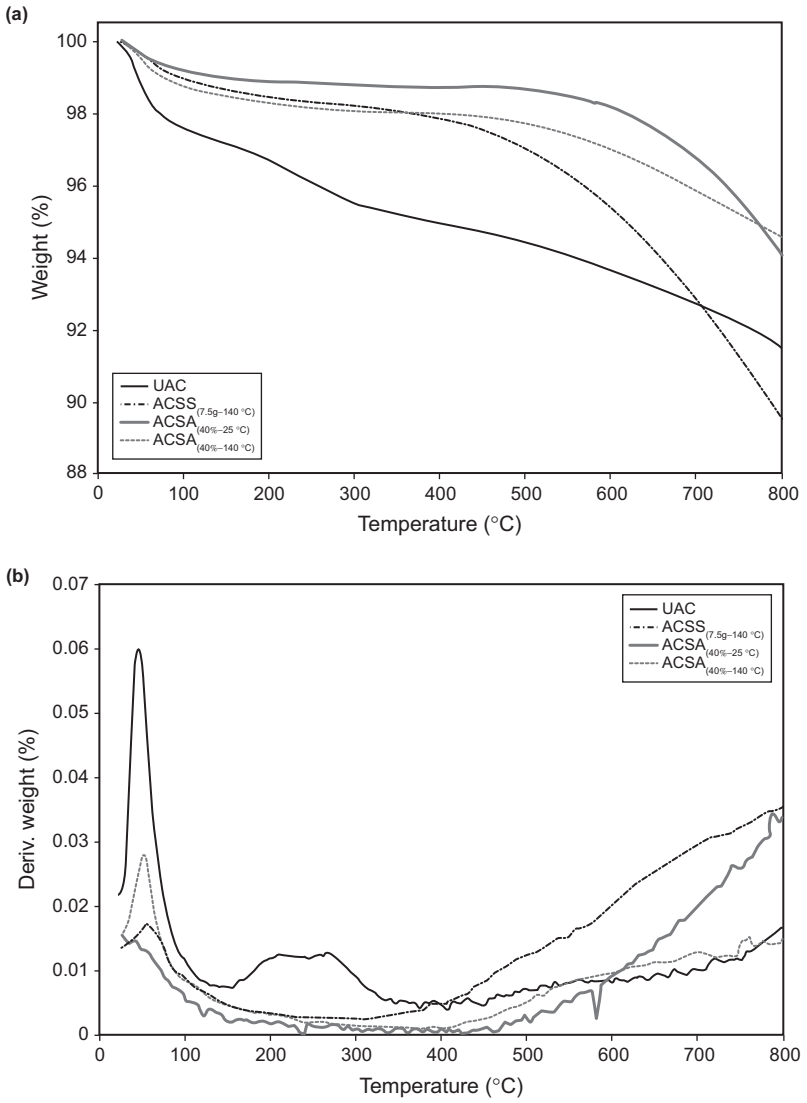

Figure 1. (a) TG and (b) DTG curves under nitrogen flow for UAC, $ACSS_{(7.5g\text{-}140\ °C)}$, $ACSA_{(40\%\text{-}25\ °C)}$ and $ACSA_{(40\%\text{-}140\ °C)}$.

activated carbon (UAC) shows two different processes of weight loss with different rates. The first stage begins at approximately 125 °C with a constant rate, which could be associated to the evaporation of adsorbed water. The second stage of weight loss starts at 400 °C, and it can be assigned to the initiation of a progressive decomposition of the carbon. The complete decomposition starts at temperatures greater than or equal to 800 °C, with a weight loss that does not exceed 15%. Therefore, the temperature of the modification treatment was fixed at 700 °C.

The TG-DTG profiles of the modified carbons are similar to the parent carbon profile. There are two weight loss steps. The first step at temperature lower than 100 °C can be attributed to the loss of adsorbed water and other volatile compounds. The weight loss at temperature higher than

500 °C indicates the beginning of the carbon decomposition. Moreover, it can be seen that the samples show different weight losses at higher temperatures, which does not exceed 20% in any case. The $ACSA_{(40\%\text{-}140\ °C)}$ sample exhibits the lowest weight loss of all the samples, whereas the $ACSS_{(7.5g\text{-}140\ °C)}$ sample shows the largest one.

3.2. Characterization of the Porous Texture

The nitrogen adsorption–desorption isotherms at –196 °C for all the samples are shown in Figure 2(a). In addition, Table 1 reports the mean and standard deviation values of the 'apparent' surface area (S_{BET}), the mesoporous volume (V_{meso}) and the volume of narrow micropores (V_n) obtained from CO_2 adsorption.

All the samples exhibit a combination of Type I and Type IV isotherms, characteristic of mesoporous adsorbents with a certain degree of microporosity. Thus, they show a high adsorption

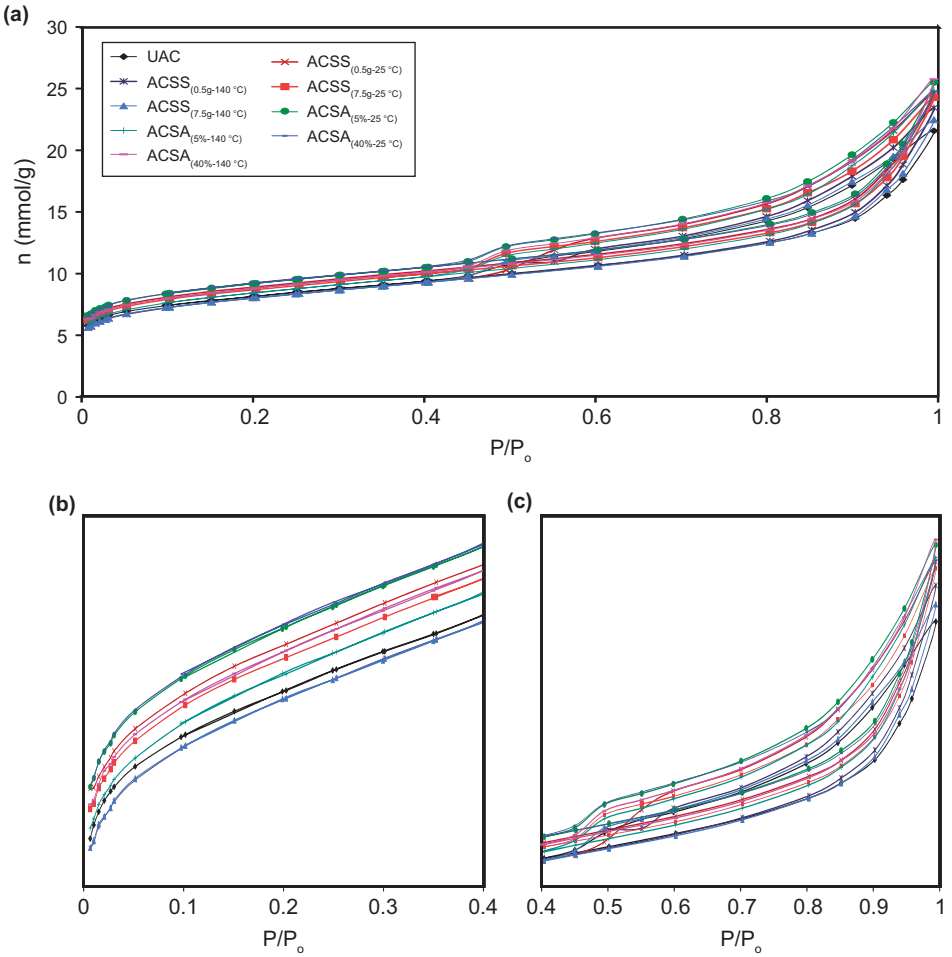

Figure 2. Nitrogen adsorption–desorption isotherms at –196 °C for all the activated carbons (a) over the whole relative pressures range and (b) between 0 and 0.4 and (c) between 0.4 and 1.

TABLE 1. Textural Properties of the Parent and Modified Activated Carbons

Samples	S_{BET} (m^2/g)	V_n (cm^3/g)	V_{meso} (cm^3/g)
UAC	589 (6)*	0.25 (0.01)	0.49 (0.01)
$ACSS_{(0.5g\text{-}25\ °C)}$	662 (5)	0.29 (0.01)	0.57 (0.01)
$ACSS_{(0.5g\text{-}140\ °C)}$	601 (4)	0.26 (0.02)	0.56 (0.01)
$ACSS_{(7.5g\text{-}25\ °C)}$	644 (5)	0.28 (0.01)	0.57 (0.02)
$ACSS_{(7.5g\text{-}140\ °C)}$	599 (6)	0.25 (0.01)	0.52 (0.01)
$ACSA_{(5\%\text{-}25\ °C)}$	680 (4)	0.29 (0.01)	0.59 (0.02)
$ACSA_{(5\%\text{-}140\ °C)}$	629 (6)	0.27 (0.01)	0.60 (0.01)
$ACSA_{(40\%\text{-}25\ °C)}$	684 (5)	0.29 (0.01)	0.56 (0.01)
$ACSA_{(40\%\text{-}140\ °C)}$	657 (5)	0.28 (0.01)	0.61 (0.01)

*Standard deviation.

S_{BET}, V_n and V_{meso} are, respectively, the 'apparent' surface area calculated by application of the BET method, the volume of narrow micropores and the volume of mesopores.

capacity at low relative pressures [Figure 2(b)], along with a hysteresis loop at relative pressures between 0.4 and 1 related to the capillary condensation in slit-shaped mesopores (Martín-Martínez 1990), as can be seen in Figure 2(c).

It can be concluded from the adsorption isotherms in Figure 2 and data in Table 1 that the performed impregnation treatments slightly modify the textural properties of the parent activated carbon, although a small increase of BET surface area is observed in samples impregnated with H_2SO_4. Thus, the samples $ACSA_{(5\%\text{-}25\ °C)}$ and $ACSA_{(40\%\text{-}25\ °C)}$ exhibit the maximum S_{BET} value in the series, around 680 m^2/g. In the same way, the two impregnation procedures hardly affected the carbon microporosity, with all samples showing quite similar V_n values (0.25–0.29 cm^3/g). However, the mesoporosity did increase for all sulphur-modified samples, with a maximum value for the sample $ACSA_{(40\%\text{-}140\ °C)}$. The changes observed in the porous texture when using H_2SO_4 as the impregnating agent can be explained on the basis of the relatively oxidant character of sulphuric acid, which would act also as a post-synthesis activating agent.

3.3. TPD

The surface oxygen groups on the parent and modified activated carbons were characterized by TPD (Zielke *et al*. 1996; Hydar *et al*. 2000; Jia and Thomas 2000). The average amounts of CO and CO_2 evolved, obtained from the integration of the TPD peaks, are reported in Table 2. In general, it can be observed that the oxygen content of the parent carbon is relatively low compared with other commercial activated carbons (Ahumada *et al*. 2002; Rios *et al*. 2007; Gonçalves *et al*. 2012). The impregnation treatment with Na_2S increases the amount of the surface oxygen groups considerably, whereas the treatment with H_2SO_4 leads to a significant decrease of these groups, mainly those that decompose evolving CO_2 (carboxylic acids and anhydrides; Table 2).

Figure 3 shows the CO_2 [Figure 3(a)] and CO [Figure 3(b)] evolution profiles, as a function of temperature, for the original activated carbon (UAC), $ACSS_{(7.5g\text{-}25\ °C)}$, $ACSS_{(7.5g\text{-}140\ °C)}$ and $ACSA_{(40\%\text{-}25\ °C)}$ samples. It can be seen that $ACSS_{(7.5g\text{-}25\ °C)}$ exhibits higher amounts of CO and CO_2, compared with all the other samples. The TPD results (Table 2 and Figure 3) indicate a clear increase in the content of oxygen groups when the impregnation is carried out with Na_2S. By contrast, the TPD profiles of CO and CO_2 evolution for $ACSA_{(40\%\text{-}25\ °C)}$ carbon show that impregnation with H_2SO_4 leads, under these conditions, to the loss of oxygen groups. The TPD

TABLE 2. Amount of Oxygen Surface Groups Evolved as CO and CO_2

Sample	CO_2 (mmol/g)	CO (mmol/g)
UAC	0.056 (0.015)*	0.003 (0.002)
$ACSS_{(0.5g\text{-}25\ °C)}$	0.091 (0.012)	0.007 (0.002)
$ACSS_{(0.5g\text{-}140\ °C)}$	0.102 (0.016)	0.016 (0.004)
$ACSS_{(7.5g\text{-}25\ °C)}$	0.152 (0.020)	0.011 (0.003)
$ACSS_{(7.5g\text{-}140\ °C)}$	0.107 (0.021)	0.007 (0.002)
$ACSA_{(5\%\text{-}25\ °C)}$	0.014 (0.010)	0.002 (0.001)
$ACSA_{(5\%\text{-}140\ °C)}$	0.016 (0.009)	0.003 (0.002)
$ACSA_{(40\%\text{-}25\ °C)}$	0.021 (0.007)	0.003 (0.001)
$ACSA_{(40\%\text{-}140\ °C)}$	0.015 (0.009)	0.003 (0.001)

*Standard deviation.

profiles of all the carbons reveal the presence of two different oxygen groups; the first one evolves CO_2 and the second leads to CO. The latter evolutes at temperatures ranging from 700 to 1000 °C, and is less abundant than CO_2, which evolutes at lower temperatures (450–900 °C). The TPD profile of the $ACSS_{(7.5g\text{-}25\ °C)}$ sample shows two CO_2 evolution peaks at 200 and 600 °C. The first one starts at 175 °C, with a band shape extending over a large temperature range, up to 300 °C. This peak can be assigned to the decomposition of the less stable groups such as carboxylic acids. The second peak, at 600 °C, is better defined, and it may be attributed to the most thermally stable structures (i.e. lactones and/or carboxylic anhydrides). At approximately 750 °C, this peak is progressively converted into a broad band, indicating the intensification of the thermal decomposition of carbons to lactones and carboxylic anhydrides (Rodríguez-Reinoso and Molina-Sabio 1998; Figueiredo *et al*. 1999). $ACSS_{(7.5g\text{-}140\ °C)}$ exhibits a very similar CO_2 evolution profile, with three decomposition processes at practically the same temperatures. However, the intensities of the peaks are different from those obtained with the same sample treated at 25 °C. Thus, while the high temperature peaks (approximately at 590 and 785 °C) are less intense than in the $ACSS_{(7.5g\text{-}140\ °C)}$ sample, the broad band at 75–325 °C is more intense, indicating the presence of a higher content of low-thermal stability oxygen groups (carboxylic groups) in this sample. By contrast, the $ACSA_{(40\%\text{-}25\ °C)}$ sample maintains the same nature of the starting oxygen groups. In fact, samples UAC and $ACSA_{(40\%\text{-}25\ °C)}$ show a CO_2 peak, at 600–800 °C, rather less intense than that corresponding to the $ACSS_{(7.5g\text{-}25\ °C)}$ sample. This peak is mainly due to the decomposition of anhydride groups, also called the high-temperature CO_2 groups (Rodríguez-Reinoso and Molina-Sabio 1998).

With regard to the CO evolution, the $ACSS_{(7.5g\text{-}25\ °C)}$ and $ACSS_{(7.5g\text{-}140\ °C)}$ samples show similar profiles as in the case of CO_2 evolution, with a single intense peak, cantered, respectively, at 888 and 866 °C. In the case of UAC and $ACSA_{(40\%\text{-}25\ °C)}$, this peak is shifted to higher temperatures (centered around 1000 °C) and is remarkably less intense than that corresponding to the $ACSS_{(7.5g\text{-}25\ °C)}$ and $ACSS_{(7.5g\text{-}140\ °C)}$ samples. In all cases, this peak can be assigned to phenol, ether and/or carboxylic/quinone groups (Rios *et al*. 2007).

In summary, the intensity of the obtained CO_2 evolution peaks confirms that the impregnation treatment with Na_2S leads to an increased amount of surface oxygen groups, while the treatment with H_2SO_4 causes an oxygen content loss, under the experimental conditions used.

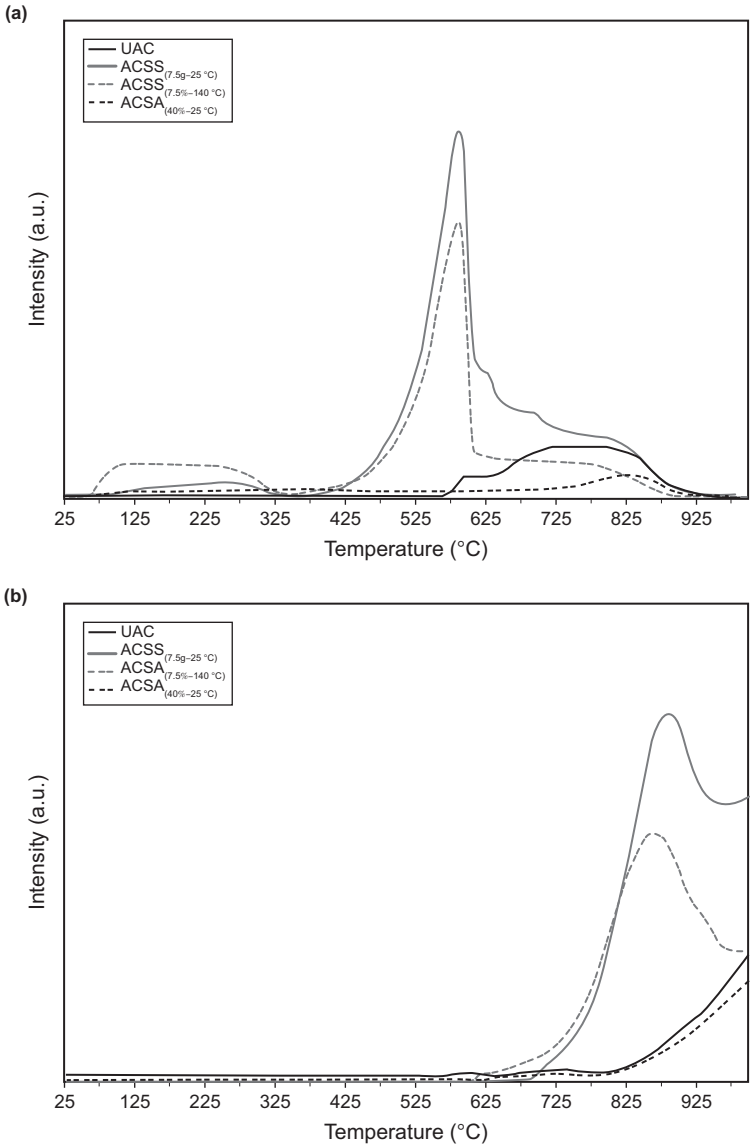

Figure 3. Temperature-programmed decomposition profiles of (a) CO_2 and (b) CO evolution for UAC, $ACSS_{(7.5g\text{-}25\ °C)}$, $ACSS_{(7.5g\text{-}140\ °C)}$ and $ACSA_{(40\%\text{-}25\ °C)}$ samples.

3.4. XPS Analysis

The surface composition of the untreated and modified activated carbons was assessed by XPS, which allows for the quantification of the different surface elements (mainly C, O and S), as well as their chemical forms (Denison *et al*. 1987). Table 3 reports the XPS mean atomic S/C ratios and the standard deviation of the values for the different adsorbents. It can be seen that the

TABLE 3. XPS Atomic S/C Ratios (at.%) of Activated Carbon Surface

Sample	S/C
UAC	–
$ACSS_{(0.5g\text{-}25\ °C)}$	0.016 (0.003)*
$ACSS_{(0.5g\text{-}140\ °C)}$	0.000
$ACSS_{(7.5g\text{-}25\ °C)}$	0.017 (0.002)
$ACSS_{(7.5g\text{-}140\ °C)}$	0.000
$ACSA_{(5\%\text{-}25\ °C)}$	0.000
$ACSA_{(5\%\text{-}140\ °C)}$	0.000
$ACSA_{(40\%\text{-}25\ °C)}$	0.022 (0.003)
$ACSA_{(40\%\text{-}140\ °C)}$	0.000

*Standard deviation.

Na_2S-impregnated samples exhibit sulphur surface only when the temperature of impregnation is 25 °C. Thus, the $ACSS_{(0.5g\text{-}25\ °C)}$ and $ACSS_{(7.5g\text{-}25\ °C)}$ samples present an atomic sulphur concentration (at.%), respectively, of 1.16 at.% (S/C = 0.016) and 1.52 at.% (S/C = 0.017). After impregnation at 140 °C, sulphur is not observed on the carbon's surface. In the case of the H_2SO_4-modified carbons, sulphur was detected only in the $ACSA_{(40\%\text{-}25\ °C)}$ sample, which exhibits the highest surface sulphur content of all the modified carbons, 2.0 at.% (S/C = 0.022).

Figure 4 shows the S 2p level XPS spectra for all sulphur-containing samples, that is, $ACSS_{(0.5g\text{-}25\ °C)}$, $ACSS_{(7.5g\text{-}25\ °C)}$ and $ACSA_{(40\%\text{-}25\ °C)}$. The same level XPS spectra corresponding to the starting material (UAC) are also included for comparison purpose. The XPS spectra are quite similar for all sulphur-containing carbons, and they show two peaks whose maximum intensities are located at, approximately 163.7 and 165 eV, which can be assigned to organic sulphur (thiol, C–SH) and elemental sulphur (–S–S– species) according to the literature (Feng *et al*. 2006; Petit *et al*. 2010; Tsubota *et al*. 2011; Mullett *et al*. 2012; Asasian *et al*. 2013; Si *et al*. 2013; Huang *et al*. 2014).

3.5. Mercury Adsorption Measurements

Figure 5 shows the Hg(II) removal capacity of the original and the modified activated carbons. The mean amount of mercury adsorbed per gram of carbon for all the samples is reported in Table 4. In the case of the sulphur-containing samples, the mean amount of Hg(II) adsorbed per mole of sulphur is also shown in the table. It can be seen that the $ACSS_{(0.5g\text{-}25\ °C)}$, $ACSS_{(7.5g\text{-}25\ °C)}$ and $ACSA_{(40\%\text{-}25\ °C)}$ samples reach a mercury removal capacity of 100% equivalent to an adsorption capacity of 0.02 mmol of Hg(II) per gram of carbon, which is an improvement above 10% in comparison with the non-modified activated carbon, which achieves the removal of 80% of Hg(II) [0.0178 mmol Hg(II)/g AC]. It should be remembered that these samples show sulphur on the surface according to the XPS data, which would indicate that the fixation of sulphur on the activated carbon surface enhances its Hg(II) adsorption capacity. However, it is difficult to directly attribute the observed improvement exclusively to the presence of sulphur and discard or minimize the contribution of the oxygen groups, whose beneficial effect in the mercury removal process from aqueous solutions is well-known. Furthermore, the porous texture of activated carbons has a direct influence on the adsorption process. Indeed, the total adsorption capacity is determined by the available surface area, defined by a well-developed porous network that is essentially constituted

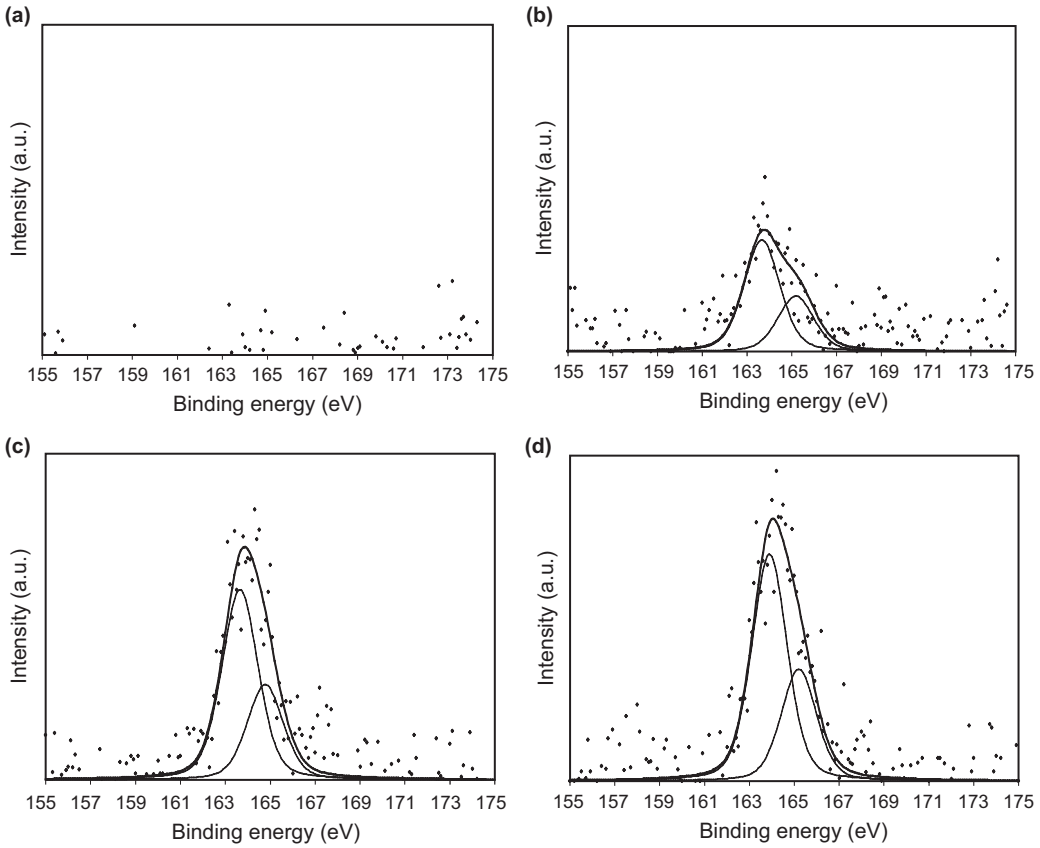

Figure 4. XPS S 2p spectra of (a) UAC, (b) $ACSS_{(0.5g\text{-}25\ °C)}$, (c) $ACSS_{(7.5g\text{-}25\ °C)}$ and (d) $ACSA_{(40\%\text{-}25\ °C)}$ samples.

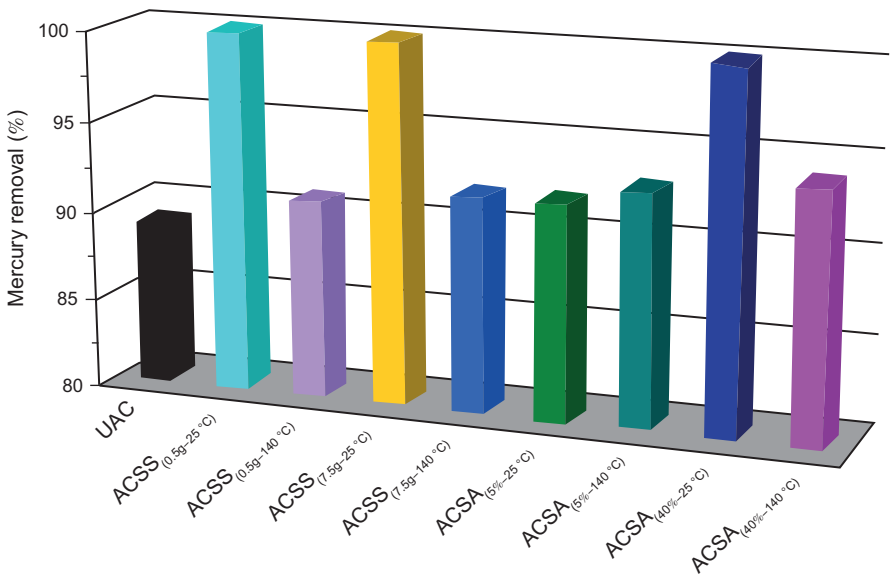

Figure 5. Mercury removal for all the samples, at 25 °C, with an initial mercury concentration of 20 mg/l and pH 2.

TABLE 4. Mercury Adsorption Capacity for All the Activated Carbons

Sample	mmol Hg(II)/g AC	mmol Hg(II)/mol S
UAC	0.0178	–
$ACSS_{(0.5g\text{-}25\ °C)}$	0.0200	0.017
$ACSS_{(0.5g\text{-}140\ °C)}$	0.0182	–
$ACSS_{(7.5g\text{-}25\ °C)}$	0.0200	0.017
$ACSS_{(7.5g\text{-}140\ °C)}$	0.0184	–
$ACSA_{(5\%\text{-}25\ °C)}$	0.0184	–
$ACSA_{(5\%\text{-}140\ °C)}$	0.0186	–
$ACSA_{(40\%\text{-}25\ °C)}$	0.0200	0.013
$ACSA_{(40\%\text{-}140\ °C)}$	0.0188	–

*Standard deviation is <0.0001.

by micropores, in which the effective adsorption process takes place, and mesopores, whose main role is to facilitate the diffusion of the mercury towards the inner porosity of the adsorbent material. Anyway, it has been found that the porous texture of the adsorbents prepared in this work is similar and thus, their different adsorptive behaviour can be attributed only to their different surface properties. As seen from the Hg(II) adsorption results, the sulphur surface content is necessary to achieve a high mercury removal from aqueous solution.

As mentioned earlier, at pH values below 4, Hg(II) is the predominant species in the aqueous solution. Several studies report that the uptake of this cation on the activated carbon surface is achieved by chemisorption (Asasian *et al*. 2013; Ie *et al*. 2013; Pillay *et al*. 2013). In the case of the unmodified carbon and the samples that do not contain sulphur, the Hg(II) adsorption may be a weak interaction between the latter and the oxygen atoms of the different oxygen-containing groups present on the carbon surface, such as carboxylic, hydroxyl and carbonyl groups, according to the following reactions (Yardim *et al*. 2003; Wahby *et al*. 2011; Pillay *et al*. 2013):

$$2C_xOH + Hg^{2+} \rightarrow (C_xO)_2Hg^{2+} + 2H^+ \quad (1)$$

$$2C_xOOH + Hg^{2+} \rightarrow (C_xCOO)_2Hg^{2+} + 2H^+ \quad (2)$$

In the case of the sulphur-containing samples, Hg(II) adsorption on the activated carbon surface occurs by the formation of a strong Hg–S bond (Pillay *et al*. 2013), which can be described as follows (Dujardin *et al*. 2000; Hadavifar *et al*. 2014):

$$2R\text{–}SH + Hg^{2+} \rightarrow R\text{–}S\text{–}Hg\text{–}S\text{–}R + 2H^+ \quad (3)$$

The latter should be the predominant mechanism in case of the $ACSA_{(40\%\text{-}25\ °C)}$ sample, which exhibits the highest surface sulphur amount and the lowest oxygen content. However, the adsorption of mercury on the surface of the $ACSA_{(0.5g\text{-}25\ °C)}$ and $ACSA_{(7.5g\text{-}25\ °C)}$ samples, having both sulphur and oxygenated groups on the surface, should take place according to both mechanisms.

In summary, the results obtained in this study show that the sulphur-modification treatments carried out on the original activated carbon lead to an improvement of the total mercury adsorption capacity. These treatments, with Na_2S and H_2SO_4, slightly modify the textural

properties of the parent activated carbon, producing a small increase in the BET surface areas, broadening existing microporosity and increasing to some extent the volume of mesopores. These modifications may influence the mercury adsorption process by facilitating the diffusion of mercury towards the micropores, and thus effectively enhancing adsorption. By contrast, an increase of the oxygen content has been observed mainly in the case of the Na_2S-treated samples at 25 °C. Oxygen surface groups are one of the key factors conditioning the mercury adsorption process. Finally, sulphur fixation on the carbon surface is necessary to achieve the total mercury adsorption capacity on these materials. In fact, the sample $ACSA_{(40\%\text{-}25\ °C)}$, even if devoid of high oxygen content, reached a 100% mercury removal. It can then be concluded that an ideal adsorbent for mercury removal should combine a well-developed porosity, a high volume of mesopores and a specifically developed surface chemistry in which oxygen groups and, specially, sulphur functionalities play the main role.

4. CONCLUSIONS

Two series of activated carbons were prepared by modification of a micro-mesoporous activated carbon by impregnation with Na_2S or H_2SO_4 aqueous solutions. These treatments produced an increase in the amount of oxygen surface groups, as evidenced by TPD measurements, which was higher for the sample treated with Na_2S at 25 °C. The surface fixation of sulphur species, mainly thiols, on activated carbon surface, was revealed by XPS analysis.

The removal of Hg(II) ions in aqueous solution by adsorption on the different carbons was effectively demonstrated. In fact, the presence of surface sulphur improved the removal capacity so that a total removal capacity of 100% was achieved. Although the roles played by the textural properties of the adsorbent and the content of oxygen surface groups should be recognized, the obtained results state the importance of the presence of surface sulphur species to obtain a high removal capacity of mercury ions in solution.

ACKNOWLEDGEMENTS

The financial support by Generalitat Valenciana, Spain (PROMETEO/2009/002) is gratefully acknowledged.

REFERENCES

Ahumada, E., Lizama, H., Orellana, F., Suárez, C., Huidobro, A., Sepúlveda-Escribano, A. and Rodríguez-Reinoso, F. (2002) *Carbon*. **40**, 2827.

Asasian, N., Kaghazchi, T., Faramarzi, A., Hakimi-Siboni, A., Asadi-Kesheh, R., Kavand, M. and Mohtashami, S.-A. (2013) *J. Taiwan Inst. Chem. Eng.,* in press, http://dx.doi.org/10.1016/j.jtice.2013.10.012.

Barán, E.J. (1994) *Química Bioinorgánica*, McGraw Hill, Madrid, Spain.

Berglund, F. and Bertin, M. (1969) *Chemical Fallout*, Thomas Publishers, Springfield, IL.

Denison, P., Jones, F.R. and Watts, J.F. (1987) *J. Phys. D: Appl. Phys*. **20**, 306.

Dujardin, M.C., Cazé, C. and Vroman, I. (2000) *React. Funct. Polym*. **43**, 123.

El Samrani, A.G., Lartiges, B.S. and Villiéras, F. (2008) *Water Res*. **42**, 951.

Feng, W., Borguet, E. and Vidic, R.D. (2006) *Carbon*. **40**, 2998.

Figueiredo, J.L., Pereira, M.F.R., Freitas, M.M.A. and Órfã, J.J.M. (1999) *Carbon*. **37**, 1379.

Garrido, J., Linares-Solano, A., Martín-Martínez, J.M., Molina-Sabio, M., Rodríguez-Reinoso, F. and Torregrosa, R. (1987) *Langmuir.* **3**, 76.
Gonçalves, A., Silvestre-Albero, J., Ramos-Fernández, E.V., Serrano-Ruiz, J.C., Órfã, J.J.M., Sepúlveda-Escribano, A. and Pereira, M.F.R. (2012) *Appl. Catal. B: Environ.* **113–114**, 308.
Gregg, S.J. and Sing, K.S.W. (1982) *Adsorption, Surface Area and Porosity*, 2nd Ed, Academic Press, London.
Griffiths, C., McGartland, A. and Miller, A. (2006) *Environ. Health Perspect.* **115**, 817.
Guo, J., Xu, W.S., Chen, Y.L. and Lua, A.C. (2005) *J. Colloid Interface Sci.* **281**, 285.
Gupta, V.K., Jain, C.K., Ali, I., Sharma, M. and Saini, V.K. (2003) *Water Res.* **37**, 4038.
Hadavifar, M., Bahramifar, N., Younesi, H. and Li, Q. (2014) *Chem. Eng. J.* **237**, 217.
Hsi, H.-C. and Chen, C.-T. (2012) *Fuel.* **98**, 229.
Huang, Y., Candelaria, S.L., Li, Y., Li, Z., Tian, J., Zhang, L. and Cao, G. (2014) *J. Power Sources.* **252**, 90.
Hydar, S., Moreno-Castilla, C., Ferro-García, M.A., Carrasco-Marin, F., Rivera-Utrilla, J., Perrard, A. and Joly, J.P. (2000) *Carbon.* **38**, 1297.
Ie, I.-R., Hung, C.-H., Jen, Y.-S., Yuan, C.-S. and Chen, W.-H. (2013) *Chem. Eng. J.* **229**, 469.
Jayson, G.G., Sangster, J.A., Thompson, G. and Wilkinson, M.C. (1984) *Carbon.* **25**, 523.
Jia, Y.F. and Thomas, K.M. (2000) *Langmuir.* **16**, 1114.
Kadirvelu, K., Kavipriya, M., Karthika, C., Vennilamani, N. and Pattabhi, S. (2004) *Carbon.* **42**, 745.
Karatza, D., Lancia, A., Musmarra, D., Pepe, F. and Volpicelli, G. (1996) *Combust. Sci. Technol.* **112**, 163.
Krishna-Murti, C.R. and Vishwanathan, P. (1991) *Toxic Metal in Indian Environment*, Tata McGraw-Hill, New Delhi, India.
Krishnan, S.V., Gullett, B.K. and Jozewicz, W. (1994) *Environ. Sci. Technol.* **28**, 1506.
Lee, S.H., Rhym, Y.J., Cho, S.P. and Baek, J.I. (2006) *Fuel.* **85**, 219.
Manchester, S., Wang, X., Kulaots, I., Gao, Y. and Hurt, R.H. (2008) *Carbon.* **46**, 518.
Martín-Martínez, J.M. (1990) *Adsorción Física de Gases y Vapores por Carbones*, Universidad de Alicante-Secretariado de Publicaciones, Alicante, Spain.
Mauchauffée, S. and Meux, E. (2007) *Chemosphere.* **69**, 763.
McKay, G. and Bino, M.J. (1990) *Environ. Pollut.* **66**, 33.
Mohan, D., Gupta, V.K., Srivastava, S.K. and Chander, S. (2001) *Colloids Surf. A: Physicochem. Eng. Asp.* **177**, 169.
Mohsem-Nia, M., Montazeri, P. and Modarress, H. (2007) *Desalination.* **217**, 276.
Mullett, M., Pendleton, P. and Badalyan, A. (2012) *Chem. Eng. J.* **211–212**, 133.
Nabais, J.V., Carrott, P.J.M. and Ribiero-Carrott, M.M.L. (2006) *Appl. Surf. Sci.* **252**, 6046.
Otani, Y., Emi, H., Kanaoka, C., Uchijima, I. and Nishino, H. (1988) *Environ. Sci. Technol.* **22**, 708.
Petit, C., Kante, K. and Bandosz, T.J. (2010) *Carbon.* **48**, 654.
Pillay, K., Cukrowska, E.M. and Coville, N.J. (2013) *Microchem. J.* **108**, 124.
Rios, R.V.R.A., Silvestre-Albero, J., Sepúlveda-Escribano, A. and Rodríguez-Reinoso, F. (2007) *Colloids Surf. A: Physicochem. Eng. Asp.* **300**, 180.
Rodríguez-Reinoso, F. and Molina-Sabio, M. (1998) *Adv. Colloid Interface Sci.* **76–77**, 271.
Si, W., Zhou, J., Zhang, S., Li, S., Xing, W. and Zhuo, S. (2013) *Electrochim. Acta.* **107**, 397.
Silvestre-Albero, A.M., Wahby, A., Silvestre-Albero, J., Rodríguez-Reinoso, F. and Betz, W. (2009) *Ind. Eng. Chem. Res.* **48**, 7125.
Tsubota, T., Takenaka, K., Murakami, N. and Ohno, T. (2011) *J. Power Sources.* **196**, 10455.
U.S. Environmental Protection Agency (EPA) (2007) *Treatment Technologies for Mercury in Soil, Waste, and Water*, Office of Superfund Remediation and Technology Innovation, Washington, DC.
Verma, V.K., Tewari, S. and Rai, J.P.N. (2008) *Bioresour. Technol.* **99**, 1932.
Wahby, A., Abdelouahab-Reddam, Z., El Mail, R., Stitou, M., Silvestre-Albero, J., Sepúlveda-Escribano, A. and Rodríguez-Reinoso, F. (2011) *Adsorption.* **17**, 603.
Wajima, T. and Sugawara, K. (2011) *Fuel Process. Technol.* **92**, 1322.
Wei, L., Radisav, D., Vidic, T. and Brown, D. (1998) *Environ. Sci. Technol.* **32**, 531.

Wenguo, F., Eric, B. and Radisav, D. (2006) *Carbon*. **44**, 2990.
Yardim, M.F., Budinova, T., Ekinci, E., Petrov, N., Razvigorova, M. and Minkova, V. (2003) *Chemosphere*. **52**, 835.
Yuan, C.-S., Lin, H.-Y., Wu, C.-H., Liu, M.-H. and Hung, C.-H. (2004) *J. Air Waste Manage. Assoc*. **54**, 862.
Zabihi, M., Ahmadpour, A. and Haghighi-Asl, A. (2009) *J. Hazard. Mater.* **167**, 230.
Zielke, U., Hüttinger, K.J. and Hoffman, W.P. (1996) *Carbon*. **34**, 983.